Electron-Temperature and Ion-Density Measurements in Partially Ionized Boundary Layer on a Flat Plate

By

Kazuoki MATSUOKA*, Haruaki KISHIGE*, Michio NISHIDA**
and Goro KAMIMOTO**

(Received March 29, 1974)

Abstract

Electron temperatures and ion densities have been measured with a cylindrical Langmuir probe in a partially ionized boundary layer flow on a flat plate. The experiments have been carried out in a low density plasma wind tunnel with argon as the test gas at local freestream Mach number of 3.5. The experimental and theoretical results have been compared, and a good agreement has been obtained for the electron temperature profile. For the ion density profile, the experimental results have qualitatively agreed fairly well with the theoretical ones.

1. Introduction

The study of an ionized gas is important to the astrophysical problem and the re-entry problem. In particular, in the problem of re-entry and related laboratory experiments, it is more realistic to consider an interaction between a partially ionized gas and a body. In view of this point, it is useful to study the structure of a boundary layer in a partially ionized gas. The boundary layer structure in the ionized gas has been experimentally studied by many workers.[1-5] Bredfeldt *et al.*[1] measured ion density profile in a flat plate boundary layer and compared the measured profile with the calculated one. Their theory was based on the assumption of a frozen flow. That is to say, the ion species concentration profile was equal to the velocity profile. The comparison between the theory and experiment indicated good agreement below about 10^{12} ions/cm^3 in a freestream. Their experiments were performed by using a shock tube. Tseng *et al.*[2] also measured the electron temperature and ion density across

* Nara Technical College (Mr. Matsuoka was studying at Kyoto University as a visiting researcher during April 1967–March 1969.)
** Department of Aeronautical Engineering.

the ionized flat plate boundary layer in a low density plasma wind tunnel by using cylindrical and flush probes. The agreements between the measured profiles of the electron temperature and ion density and the calculated ones were very good. In contrast with the theory of Bredfeldt *et al.*, Tseng *et al.* included the recombination term in the species conservation equation. The electron temperature profiles in an atmospheric pressure boundary layer were investigated by Brown *et al.*[3] Their experiments were conducted in a NaK seeded argon plasma and the population temperature was decided from the measurements of the sodium number densities in the first excited level and the ground level. By relating the measured population temperature to the electron temperature by the rate equation for the first excidet level of sodium, the comparisons between the measured and calculated electron temperature profiles were made. Using a hypersonic shock tunnel, Dunn[4] investigated the ionized flat plate boundary layer with the Langmuir probe technique. His measurement indicated that in the far downstream of the leading edge, the measured electron temperatures across the boundary layer remained constant within the experimental error. The constant electron temperatures across the boundary layer were also observed by Boyer *et al.*[5]

In the present study the electron temperature and ion density in the flat plate ionized boundary layer have been measured with a cylindrical probe and the measured profiles have been compared with the calculated ones. The flush probe on the surface of the flat plate was not used, so that the wall boundary conditions for the electron temperature and ion density have been derived from the consideration of a collisionless sheath. Such wall conditions are able to be decided once a freestream condition is known. It is the purpose of this paper to compare the experimentally obtained electron temperature and ion density profiles with the theory developed for the collision-less sheath consideration.

2. Theoretical Considerations

2.1 Preliminary Discussion

We consider the nonequilibrium laminar boundary layer on a flat plate where a gas is partially ionized. In the case of partially ionized gas, a sheath formed next to the wall is thin compared with the boundary layer thickness, so that ionized gas in the boundary layer is electrically neutral. Therefore, since ions move with electrons, the concept of ambipolar diffusion can be adopted. If a flat plate is electrically insulated from the tunnel wall, or if electric field is not applied to it, it will be at floating potential. Since it is generally lower than plasma potential, an ion sheath is formed, so that only the electrons which overcome the potential difference between the wall and

the plasma can reach the wall in addition to the ions. However, the net current normal to the wall must be zero. In accordance with the above-mentioned boundary layer model, we make the following assumptions:

(1) The gas is composed of argon atoms, ions and electrons.
(2) The degree of ionization $\ll 1$.
(3) There are no external magnetic and electric fields in the flow.
(4) Ions are in thermal equilibrium with atoms everywhere, $T_A=T_I$.
(5) Steady flow, $\partial/\partial t=0$.
(6) Free stream conditions constant along x.
(7) Collision-less sheath.
(8) Ambipolar diffusion, $n_E=n_I$, $V_{dE}=V_{dI}$.

2.2 Basic Equation

Based on the above assumption (2), the over-all conservation equations are not coupled with the basic equations for the charged species, so that the basic equations to be solved here are the electron-ion continuity and electron energy equations. When we use the coordinate system as shown in Fig. 1, the basic equations are written in the following form:[6]

Conservation of electron-ion pair:

$$\rho u\frac{\partial c}{\partial x}+\rho v\frac{\partial c}{\partial y}=\frac{\partial}{\partial y}\left(\rho D_a\frac{\partial c}{\partial y}\right)+\dot{W} \tag{1}$$

Conservation of electron energy:

$$\frac{\partial}{\partial x}\left(\frac{3}{2}n_E kuT_E\right)+\frac{\partial}{\partial y}\left(\frac{3}{2}n_E kvT_E\right)=\frac{\partial}{\partial y}\left(\lambda_E\frac{\partial T_E}{\partial y}-\rho C_E V_{dE}h_E\right)$$
$$-n_E kT_E\left(\frac{\partial u}{\partial x}+\frac{\partial v}{\partial y}\right)+R+L \tag{2}$$

where

(1) C: the concentration of the electron-ion pair, expressed as

$$C=(\rho_I+\rho_E)/\rho\cong\rho_I/\rho$$

(2) ρ: the density
(3) m: the mass

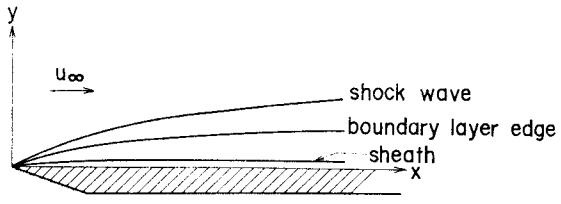

Fig. 1. Coordinate system.

(4) D_a: the ambipolar diffusion coefficient

(5) n: the number density

(6) T: the temperature

(7) V_a: the ambipolar diffusion velocity

(8) h_E: the electron enthalpy

(9) the subscripts E and I represent the electrons and the ions, respectively.

When the electron-electron and electron-ion collisions predominate over the electron-atom collisions, R, the energy transfer rate due to elastic collisions, and λ_E, the thermal conductivity of the electrons, are, respectively, of the form[7]

$$R=12\sqrt{2}\,n_E^2\left(\frac{m_E R T_E}{\pi}\right)^{1/2}\left(\frac{k(T_A-T_E)Q_{EE}}{m_A}\right) \tag{3}$$

$$\lambda_E=\frac{75k}{64(1+\sqrt{2})Q_{EE}}\left(\frac{\pi k T_E}{m_E}\right)^{1/2} \tag{4}$$

where the subscript A represents the atoms, and Q_{EE} is the Coulomb cross section. In Eq. (1), $\dot{W}$ is the mass production rate of the electron-ion pair. Under the condition considered here, further ionization in the boundary layer is negligible compared with the recombination of a pre-ionized gas so that $\dot{W}$ is expressed as

$$\dot{W}=-\beta m_I n_E^2 \tag{5}$$

where β is the recomnination coefficient. Chen[8] calculated the recombination coefficient of argon using Gryzinski's formula for the electron-atom collision process. The calculated results were compared with the measured ones in a decaying plasma produced by a transient plasma, and a good agreement was obtained. Using Chen's results, we make an approximate expression for the recombination coefficient of argon over the range $1000°\mathrm{K}\leq T_E\leq 4000°\mathrm{K}$ and $10^{11}\,\mathrm{cm}^{-3}\leq n_E\leq 10^{14}\,\mathrm{cm}^{-3}$. It can be expressed by the double series

$$\log_{10}\beta=\sum_{i=0}^{3}\sum_{j=0}^{2}A_{ij}\left[\log_{10}\frac{n_E(\mathrm{cm}^{-3})}{10^{11}}\right]^i\left[\frac{1000}{T_E(°\mathrm{K})}\right]^{j/2} \tag{6}$$

This procedure is the same as done by Talbot *et al.*[9] for hydrogen. Solving the resulting matrix equation, we have

$A_{00}=-12.88$	$A_{01}=\ 2.074$	$A_{02}=\ 1.337$
$A_{10}=-2.874$	$A_{11}=\ 9.133$	$A_{12}=-5.259$
$A_{20}=-1.160$	$A_{21}=-2.681$	$A_{22}=\ 1.521$
$A_{30}=-0.1536$	$A_{31}=\ 0.3513$	$A_{32}=-0.1977$

The energy transfer rate due to in-elastic collision, L, is expressed as

$$L=\beta n_E^2 E \tag{7}$$

For an optically thin argon plasma, Chen[10] calculated E. According to his result,

E can be expressed approximately as

$$E=(2/3)(n_E/10^{13}-0.1)+0.9 \qquad (\text{in } eV) \tag{8}$$

2.3 Boundary Conditions

It is well known that the development of a viscus boundary layer near the surface of the plate serves to generate a shock wave in the flow field. Using the theory by Stewartson[11], we analyzed the effect of the shock under our experimental conditions. As for results, the value of the hypersonic interaction parameter, $\bar{\chi}=M^3/\sqrt{Re_e}$, is about 7 at the measuring location, and the pressure interaction is fairly weak.

The boundary conditions at the outer edge of the boundary layer are

$$C(\infty)=C_e, \qquad T_E(\infty)=T_{E_e} \tag{9}$$

where the suffix e denotes the condition at the outer edge of the boundary layer. The boundary conditions at the wall for the electron temperature and the mass fraction of the electron-ion pair are determined as follows:[6]

For the present problem, where the wall is at floating potential, the net current density normal to the wall is zero and therefore

$$n_{E_{sh}}e\frac{\langle V_E\rangle}{4}\exp\left(-\frac{e\Delta\phi}{kT_{E_{sh}}}\right)-n_{I_{sh}}eV_I=0 \tag{10}$$

Next a relation is obtained from the continuity of the mass flow of the ions at the edge of the sheath and therefore

$$\left(\rho D_a\frac{\partial c}{\partial y}\right)_{sh}=\rho_{sh}C_{sh}V_I \tag{11}$$

A third relation is obtained from the continuity of electron energy flux through the outer edge of the sheath and therefore

$$\left(\lambda_E\frac{\partial T_E}{\partial y}\right)_{sh}-(\rho c_E V_{dE}h_E)_{sh}$$
$$=\{2kT_{E_{sh}}+e(\phi_{sh}-\phi_w)\}\frac{n_{E_{sh}}}{4}\langle V_E\rangle\exp\left\{-\frac{e(\phi_{sh}-\phi_w)}{kT_{E_{sh}}}\right\} \tag{12}$$

where $\langle V_E\rangle=(8kT_{E_{sh}}/\pi m_E)^{1/2}$ and $V_I=(kT_{E_{sh}}/m_I)^{1/2}$.

Since the sheath is very thin compared with the boundary layer thickness, these boundary conditions may be taken to be the boundary conditions at the wall.

2.4 Coordinate Transformation

In order to obtain a similar solution, the following transformation of coordinates is introduced:

$$\xi(x)=x, \quad \eta(x,y)=\left(\frac{u_e}{\rho_e\mu_e\xi}\right)^{1/2}\int_0^y\rho dy \tag{13}$$

The over-all continuity equation is identically satisfied if we define a stream function ψ such that $\partial\psi/\partial y=\rho u$ and $\partial\psi/\partial x=-\rho v$. By defining the dimension-less stream function $f=\psi/(\rho_e\mu_e u_e\xi)^{1/2}$, $\partial f/\partial\eta=u/u_e$ can be easily obtained. The following dimension-less quantities are introduced:

$$\theta=\frac{T_A}{T_{A_e}},\quad Z=\frac{c}{c_e},\quad \Theta=\frac{T_E}{T_{E_e}} \tag{14}$$

By using Eqs. (1)–(2) and assuming local similarity, $\partial/\partial\xi=0$, the conservation equations are rewritten as follows:

Conservation of electron-ion pair:

$$\left(\frac{l}{S_{ca}}Z'\right)'+\frac{1}{2}fZ'=\xi\frac{n_{E_e}}{u_e}\frac{Z^2}{\theta}\beta \tag{15}$$

Conservation of electron energy:

$$\Theta''+\left(\frac{5}{2}\frac{\Theta'}{\Theta}-\frac{\theta'}{\theta}+\frac{a}{2}\frac{Z\theta f}{\Theta^{5/2}}\right)\Theta'+\frac{a}{3}\frac{\theta f}{\Theta^{5/2}}\left(\frac{3}{2}Z'+\frac{Z\theta'}{\theta}\right)\Theta$$
$$+b\xi\frac{Z^2}{\Theta^4}\left(\frac{\theta}{\tau}-\Theta\right)+b\xi\left(1-\frac{1}{\tau}\right)\frac{\beta}{\beta_e}\frac{Z}{\theta}=0 \tag{16}$$

where l is the Chapman-Rubesin constant, τ is expressed as T_{Ee}/T_{Ae}, ξ is treated as parameter and the Joule heating is ignored, and ( )′ denotes the derivative with respect to η, and

$$a=\frac{3(1+\sqrt{2})}{3}P_r c_e\frac{\varepsilon}{\tau^{1/2}}\frac{Q_{EE_e}}{Q_{AA_e}} \tag{17}$$

$$b=\frac{256(2+\sqrt{2})}{25\pi}\frac{\mu_e}{\rho_e u_e}(\varepsilon Q_{EE_e}n_{I_e})^2 \tag{18}$$

where μ is the viscosity, ε is expressed as $(m_E/m_A)^{1/2}$, and S_{ca} is the ambipolar Schmidt number expressed as[12)]

$$S_{ca}=\frac{2.51}{1+T_E/T_A}\frac{T_A+11.5T_A^{1/2}}{T_A+142} \tag{19}$$

The boundary conditions for z and Θ are rewritten as

$$Z(\infty)=1,\qquad \Theta(\infty)=1 \tag{20}$$

$$Z'(0)=S_{ca}(0)R_{e_e}^{1/2}\left(\frac{V_I}{u_e}\right)\frac{1}{\theta^{0.816}}Z(0) \tag{21}$$

$$\Theta'(0)=\frac{64(1+\sqrt{2})}{75\pi}\left[-\frac{1}{2}-\frac{1}{2}\log_e(2\pi)-\log_e\varepsilon\right]\left(\frac{\mu_e}{\rho_e u_e}\right)^{1/2}$$
$$\times\varepsilon n_{I_e}Q_{EE_e}\xi^{1/2}\frac{Z(0)}{\Theta(0)} \tag{22}$$

where R_e is the Reynolds number.

By solving the transformed equations for the conservations of the over-all momentum and energy which are decoupled with the charged particle equations, f and θ are determined.

3. Numerical Calculations

In order to compare the measured profiles with the theoretical ones, the profiles of the electron temperature and ion density have been numerically calculated. For the purpose of simplicity of the analysis, $P_r=2/3$ and $l=1$ are taken. Since both of Eqs. (15) and (16) are coupled and nonlinear, iteration procedures are necessary to solve them. First, we obtain the solutions of f and θ by solving the over-all basic equations. These solutions are used in Eqs. (15) and (16). In the second stage, by taking $S_{ea}=1$ and neglecting the mass production term in Eq. (15), an analytical solution of z can be easily obtained, which corresponds to the chemically frozen solution. Using this solution in Eq. (16), the approximate solution of Θ can be determined. Using the solution of Θ in Eq. (16), the approximate solution of z is obtained. Thus, the iteration is carried out. All computations using the Runge-Kutta-Gill method have been performed on the digital computer FACOM 230-75.

4. Experimental Procedure

Experiments have been performed in a low density plasma wind tunnel as shown in Fig. 2. A detailed description of this test facility and its associated instrumentation has been already reported[13]. Therefore we give only an outline of it here. It is a continuous wind tunnel with a vacuum pump drive. A test gas is heated and partially

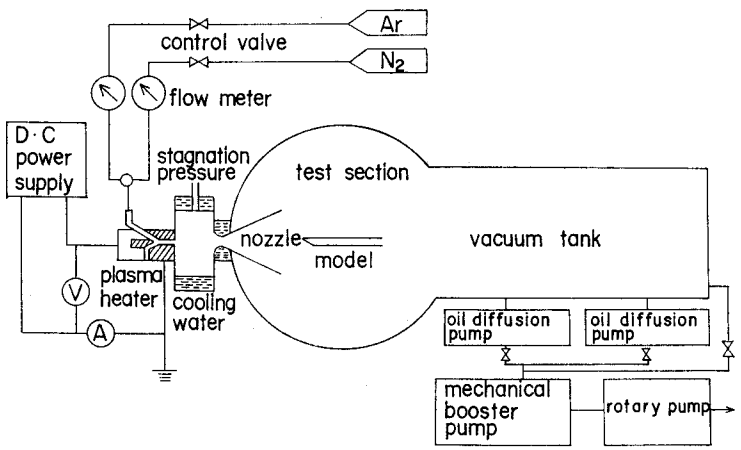

Fig. 2. Schematic of a plasma jet wind tunnel.

Table 1. Experimental conditions.

Cooland	water	helium gas	liquid nitrogen
argon mass flow rate (gr/sec)	0.099		
stagnation pressure (mm Hg)	5.77		
pressure in test section (mm Hg)	0.030		
Mach number	3.5		
degree of ionization	1.1×10^{-3}	1.2×10^{-3}	1.3×10^{-3}
n_{Ae} (cm^{-3})	1.8×10^{15}	1.8×10^{15}	1.8×10^{15}
n_{Ee} (cm^{-3})	1.9×10^{12}	2.1×10^{12}	2.3×10^{12}
T_{Awe} (°K)	300	390	220
T_{Ae} (°K)	540	530	550
T_{Ee} (°K)	1400	1300	1500
u_e (cm/sec)	1.5×10^{5}	1.5×10^{5}	1.5×10^{5}
R_{e_e}	440	440	420

ionized by a dc arc discharge with a power of 4–6 KW, and goes into a plenum chamber. Then, the test gas is expanded through a hypersonic nozzle into a test section. The plenum chamber is 77 mm in inner diameter and 90 mm in length. The diameters of a nozzle throat and exit are 13.6 mm and 50 mm, respectively. The freestream conditions are given in Table 1. The aforementioned assumptions are valid for the present conditions shown in Table 1.

Figure 3 shows the configuration of the experimental apparatus. We measured the electron temperature and the ion density in the boundary layer by traversing a

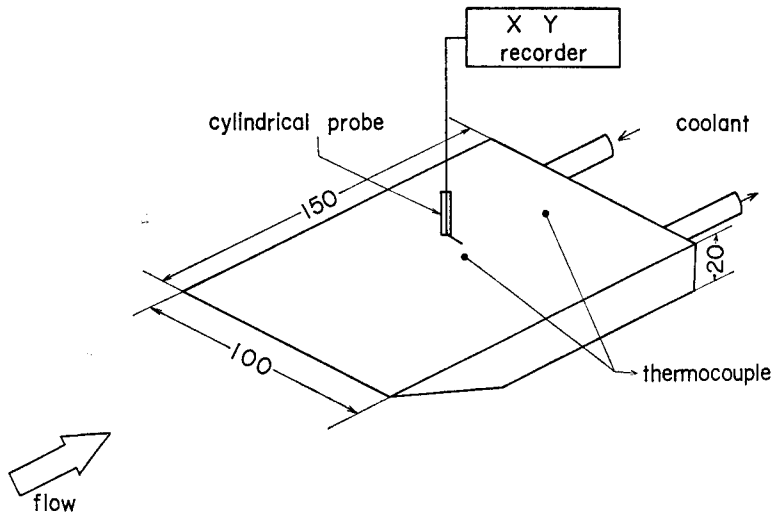

Fig. 3. Flat plate model.

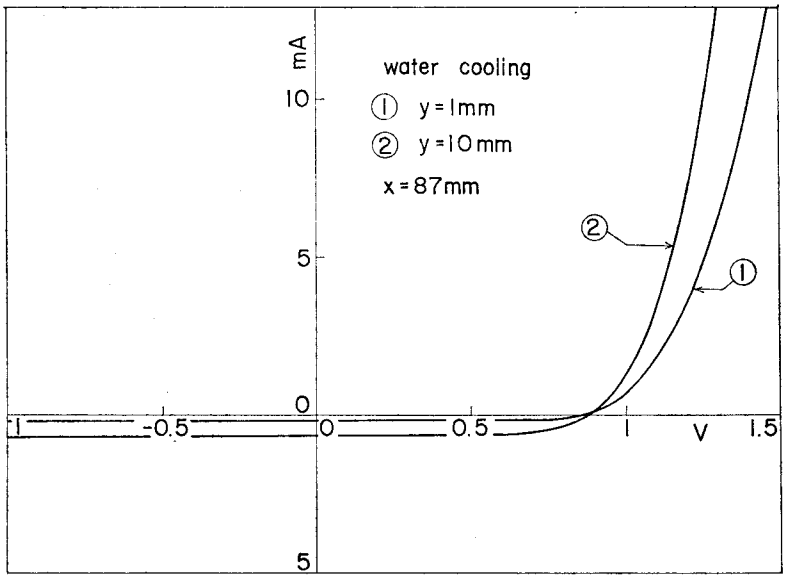

Fig. 4. Cylindrical Langmuir probe characteristics.

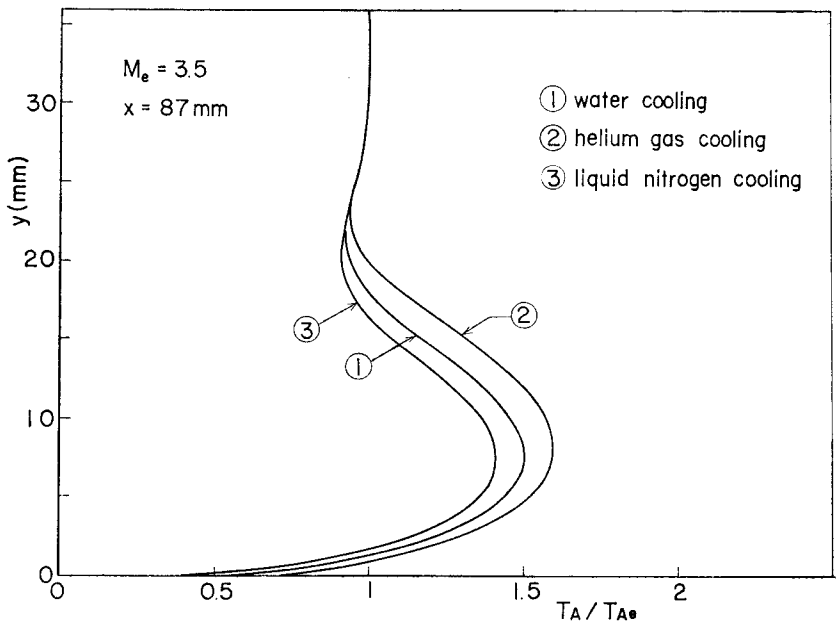

Fig. 5. Heavy-particle temperature profiles.

cylindrical probe. The current-potential characteristics could be recorded rapidly on an X–Y recorder, and these yielded immediate information on the local electron temperature and ion density. In order to investigate the effect of the wall temperature on the electron temperature and ion density profiles in the boundary layer, the experiments were carried out for three different wall temperatures which were produced by cooling the flat plate with water, helium gas and liquid nitrogen.

The flat plate model is made of brass with a sharp leading edge of an angle 22° and electrically insulated from the wall of the wind tunnel. The flat plate had a span of 100 mm, a length of 150 mm and a thickness of 20 mm. A thermo-couple installed in the flat plate supervised constancy of the surface temperature of the flat plate. During the experiments the gas flow, conditions were kept constant for the three cases as shown in Table 1. The electron temperature and ion number density profile measurements in the boundary layer flow on the flat plate were obtained with cylindrical probes setting

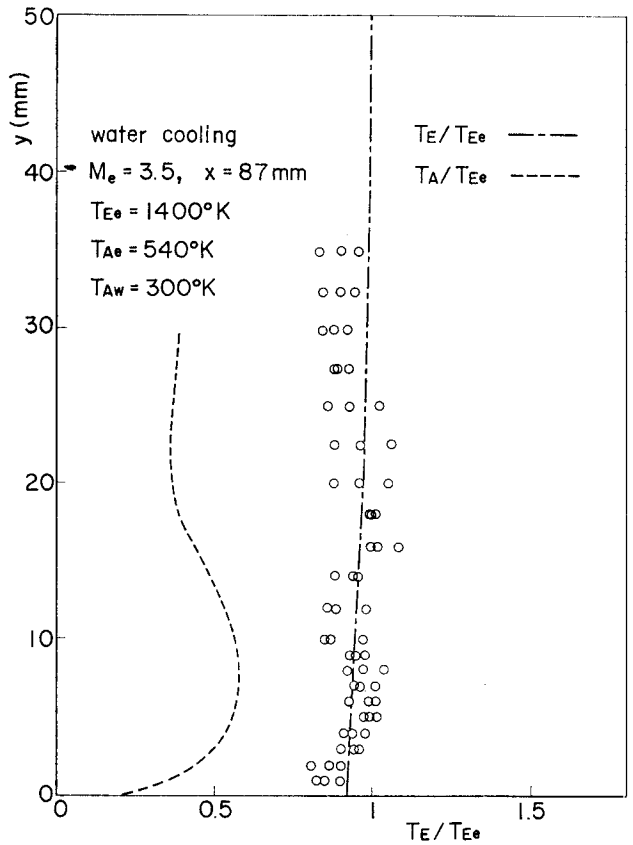

Fig. 6. Electron temperature profile when the plate is water-cooled.

in the flow direction, parallel to the plate surface. The probe was made of tungusten wire with 0.28 mm diameter and 10.40 mm length. From the current-potential characteristic record on the X–Y recorder, we obtained the electron temperature T_E and electron number density n_E, using the probe theory given by Sonin[12]. The probe potential was supplied by a battery. The voltage applied to the probe was manually altered using a variable resistance. Typical cylindrical Langmuir probe characteristics are shown in Fig. 4.

5. Experimental Results and Discussions

Figure 5 shows the heavy-particle temperature profiles in the boundary layer on the flat plate, which have been numerically calculated by taking the measured wall temperature as the wall boundary condition. The thermal layer is 25 mm for the three cases.

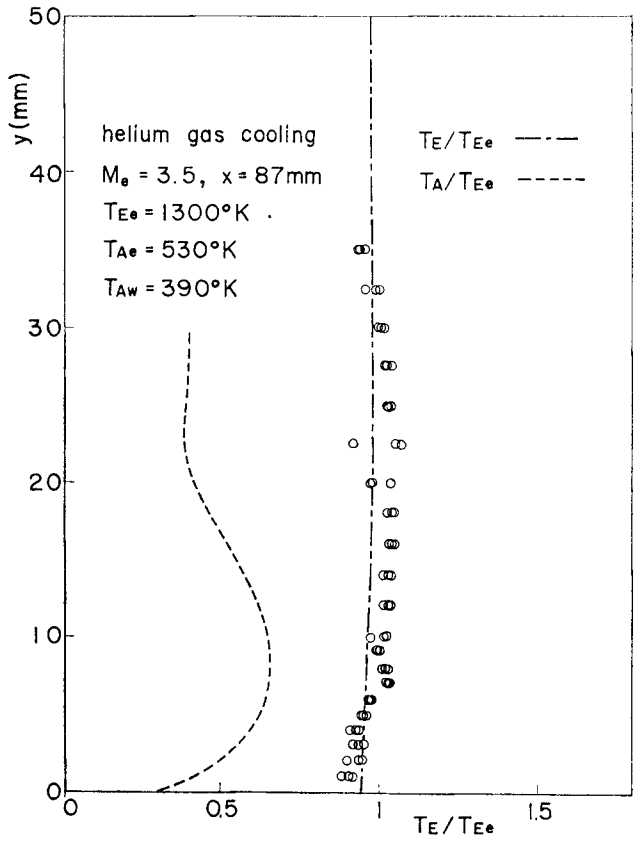

Fig. 7. Electron temperature profile when the plate is helium-cooled.

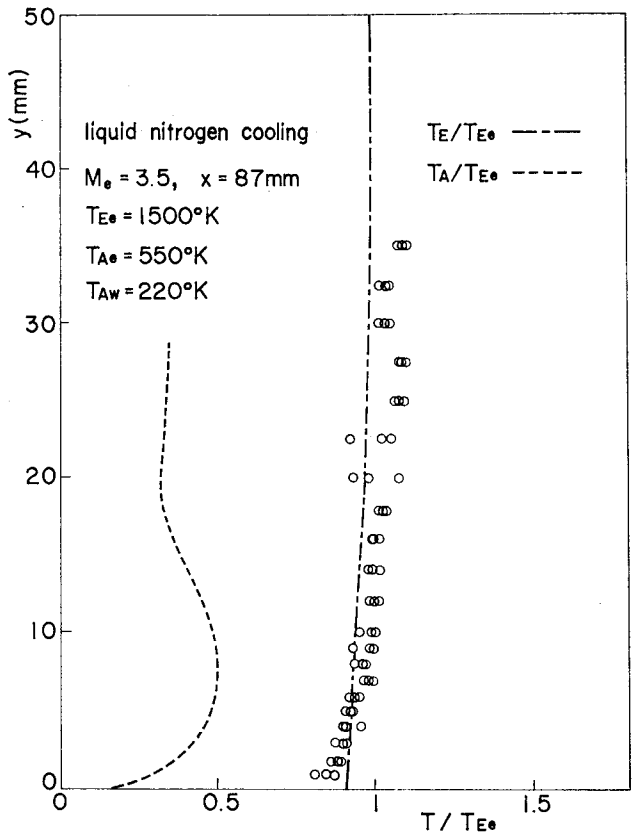

Fig. 8. Electron temperature profile when the plate is lifiuid nitrogen-cooled.

Figure 6–8 show the measured electron temperature profiles in the boundary layer on the flat plate together with the heavy-particle temperature profiles for the three cases of the surface temperature of the flat plate. The probe measurements were made at a location of 87 mm from the leading edge, where the value of the hypersonic interaction parameter, $\chi = M^3/\sqrt{Re_e}$, is about 7. It is seen from these figures that the electron temperature is significantly higher than the heavy-particles temperature, not only in the freestream but also in the boundary layer, In other words. the electrons and the heavy-particles are not in thermal equilibrium. This presumably results from the fact that the energy transfer, due to elastic collisions between the electron and the heavy-particles, is very poor. Figures 6–8 also show the comparisons between the measured electron temperature profiles and the calculated ones. The comparisons show good agreement, except for the small region near the wall for the three cases. Near the wall, the electron temperature decreases toward the wall, but except for this region it seems to remain constant. The constant electron temperature across the boundary layer was

also observed in the experiments carried out by Dunn[4] and Boyer *et al.*[5] In particular, the decrease toward the wall in the electron temperature near the wall was also observed in Boyer *et al.*'s experiments. The decrease near the wall in the electron temperature is observed in the present experiment, due to the cooling effect at the surface. The electron thermal layer has a thickness of 50 mm. According to the numerical results, the electron temperature gradient at the wall is very small, say, $(\partial T_E/\partial y)_W \simeq 0$. However, in the present experiments we could not confirm the very small gradient of the electron temperature at the wall, since a flush probe on the flat plate surface was not used. The influence of the surface temperature on the electron temperature profile in the boundary layer was investigated. However, it was not found in the range of the surface temperature accomplished here. It is expected that its effect is very small under the present conditions. Figures 9–11 show the measured ion density profiles and the calculated ones. Since the ion density at the surface was not experimentally determined, the wall condition for z has been determined with a

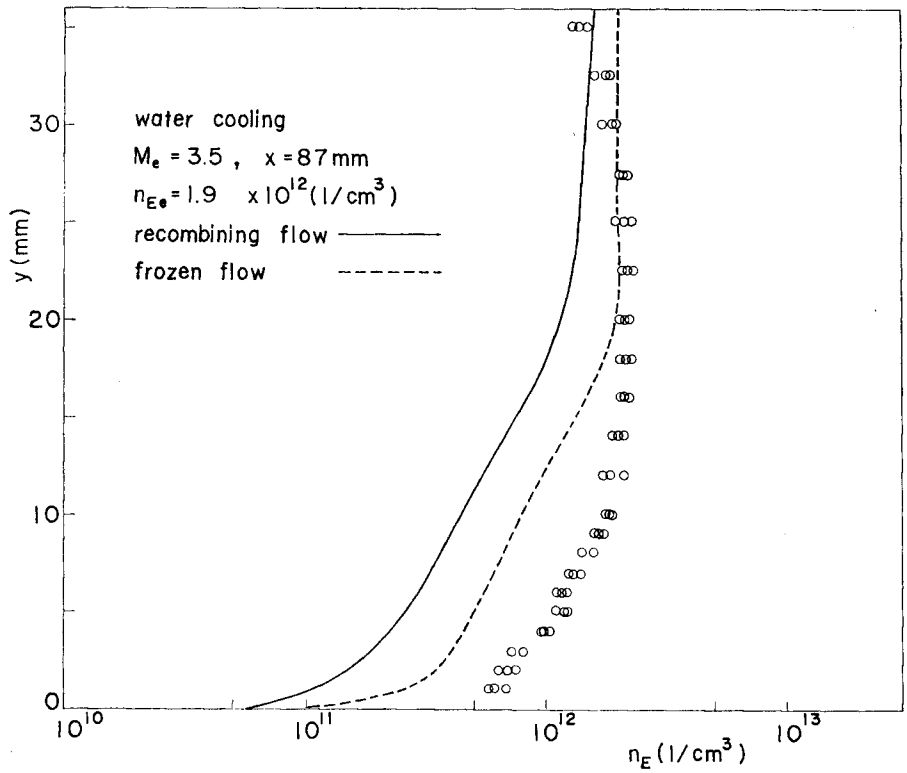

Fig. 9. Ion density profile when the plate is water-cooled.

shooting method. The measured ion densities in the boundary layer are considerably larger than the calculated ones for both cases of a chemically frozen flow and a recombining flow. It is seen from these figures that the measured ion density profiles are similar to the calculated ones for the frozen flow rather than for the recombining flow. However, the experimental and numerical results are qualitatively in good agreement.

6. Concluding Remarks

The cylindrical Langmuir probe has been applied in studying the charged species properties in the flat plate boundary layer of a partially ionized argon. Numerical solutions to the charged species equations in the quasi-neutral region of the boundary layer have been also presented in order to be compared with the experimental results. The results are as follows:

(1) The electrons are in thermal nonequilibrium with the heavy-particles not only in the freestream but also in the boundary layer.

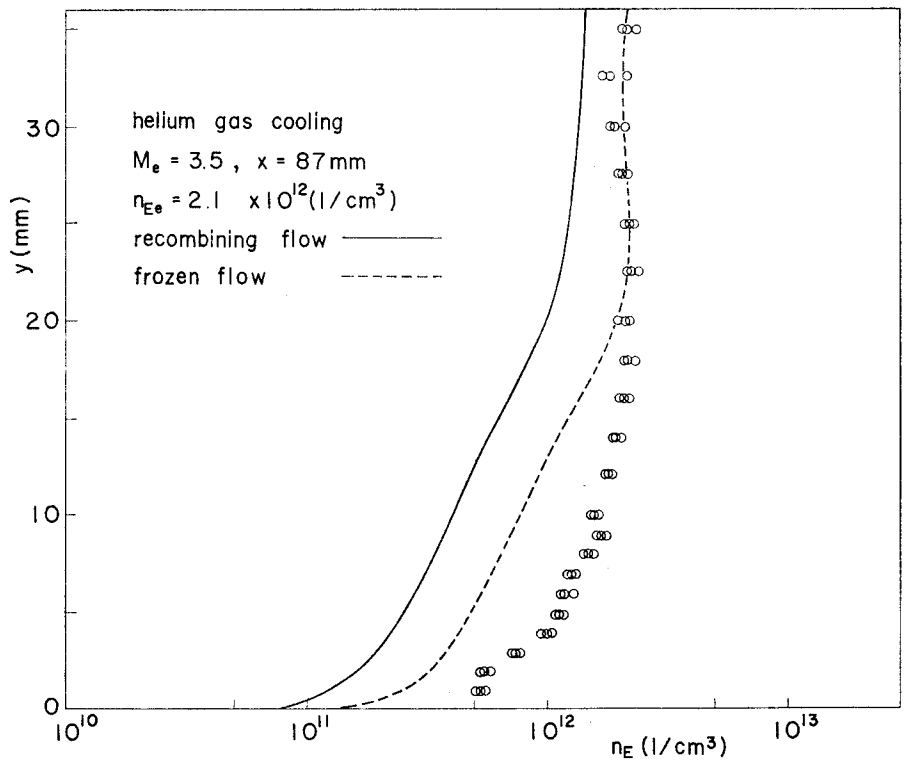

Fig. 10. Ion density profile when the plate is helium-cooled.

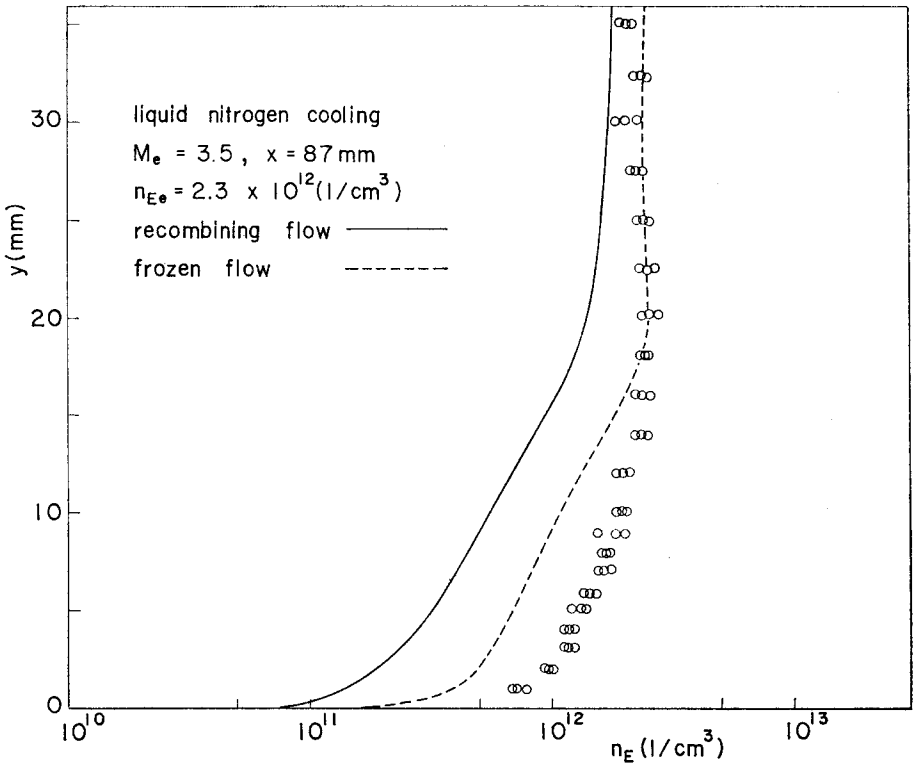

Fig. 11. Ion density profile when the plate is liquid nitrogen-cooled.

(2) The electron temperature does not change so significantly as the heavy-particle temperature in the boundary layer.

(3) The electron thermal layer is very thick compared with the heavy-particle thermal layer.

(4) The variation of the electron temperature in the boundary layer is very small.

(5) The measured electron temperature profiles are in good agreement with the calculated ones excepting the small region near the wall.

(6) The measured ion density profiles qualitatively agree with the calculated ones for the frozen flow.

(7) The effect of the surface temperature on the electron temperature profile is not observed in the range of the surface temperatures accomplished here.

References

1) Bredfeldt, H. R., Scharfman, W. E., Guthart, H. and Morita, T., AIAA J., Vol. 5 (1967), 91.
2) Tseng, R. C. and Talbot, L., AIAA Paper, No. 70-86 (1970); also AIAA J., Vol. 9 (1971), 1365.
3) Brown, R. T. and Mitchner, M., Phys. Fluids, Vol. 14 (1971), 933.

4) Dunn, M. G., AIAA J., Vol. 9 (1971), 1561.
5) Boyer, D. W., Touryan, K. J. and Russo, A. J., AIAA Paper, No. 72-104; also AIAA J., Vol. 10 (1972), 1667.
6) Nishida, M. and Matsuoka, K., AIAA J., Vol. 9 (1971), 2117.
7) Jaffrin, M. Y., Phys. Fluids, Vol. 8 (1965), 606.
8) Chen, C. J., J. Chem. Phys., Vol. 50 (1969), 1560.
9) Talbot, L., Chou, Y. S. and Roben, F., Institute of Engineering Research, University of California, Berkeley, Report, No. AS-65-14 (1965).
10) Chen, C. J., Phys. Rev., Vol. 163 (1967-, 1.
11) Stewartson, K., J. Aero. Sci., Vol. 22 (1955), 303.
12) Sonin, A. A., Institute for Aerospace Studies, Toronto University, UTIAS Report, 109 (1965).
13) Kamimoto, G., Kimura, T. and Teshima, K., Dept. of Aero. Eng., Kyoto Univ., C. P. 7 (1965).